(Preprint) AAS 10-XXX

ADVANCED NAVIGATION STRATEGIES FOR ASTEROID SAMPLE RETURN MISSIONS

K. Getzandanner,* J. Bauman,† B. Williams,† J. Carpenter*

Flyby and rendezvous missions to asteroids have been accomplished using navigation techniques derived from experience gained in planetary exploration. This paper presents analysis of advanced navigation techniques required to meet unique challenges for precision navigation to acquire a sample from an asteroid and return it to Earth. These techniques rely on tracking data types such as spacecraft-based laser ranging and optical landmark tracking in addition to the traditional Earth-based Deep Space Network radio metric tracking. A systematic study of navigation strategy, including the navigation event timeline and reduction in spacecraft-asteroid relative errors, has been performed using simulation and covariance analysis on a representative mission.

INTRODUCTION

The NEAR Shoemaker spacecraft was placed into orbit and soft-landed on the surface of the asteroid 433 Eros in February 2001, using a navigation strategy that relied on a combination of Deep Space Network (DSN) radio metric tracking and optical landmark tracking obtained from on-board imagers. Although it also carried a laser ranging instrument, the ranging data were used for asteroid model improvements and trajectory reconstruction, and thus it did not directly impact trajectory estimates used for propulsive maneuvers. In the final hours leading up to landing, the ranging data were down-linked for real-time monitoring of slant range to the surface, but it was not used to influence the landing sequence. In addition, NEAR Shoemaker did not include any navigation autonomy to change or abort the landing sequence once it had been initiated by ground command. Although the scenario was successfully used for landing NEAR Shoemaker, the mission risk for a sample return mission can be reduced by processing the additional slant range information with an appropriate level of on board autonomous navigation. On the other hand, the Hayabusa mission provides an example of proximity operations for an asteroid sample return using in situ ranging and a high level of on board autonomous navigation; however, onboard navigation issues were encountered that increased mission risk and produced uncertainty that a sample was obtained.

This paper presents analysis of advanced navigation strategies required to meet the unique challenges for precision navigation to acquire a sample from an asteroid and return it to Earth. These strategies rely on tracking data types such as spacecraft-based laser ranging and optical landmark tracking in addition to the traditional Earth-based Deep Space Network radio metric tracking. A systematic study of navigation strategy during the proximity operations, including

* NASA Goddard Space Flight Center, Navigation & Mission Design Branch, Greenbelt, Maryland 20771
† KinetX, Inc, Space Navigation and Flight Dynamics Practice, Simi Valley, California 93065

the navigation event timeline and reduction in spacecraft-asteroid relative errors, is performed using simulation and covariance analysis for a representative mission. In these studies, the proper balance between ground-based navigation and on board autonomous navigation is determined by studying the evolution of the uncertainty in the relevant dynamic parameters. These parameters include the spacecraft position and velocity relative to the asteroid and the asteroid spin state and gravity. The uncertainty in these parameters is relatively large early in the encounter and rendezvous phases, and is progressively lowered during survey and mapping phases until the landing and sample acquisition can be attempted. Monte Carlo simulations are used to demonstrate these strategies for an asteroid sample return mission.

PROBLEM STATEMENT

The objective of this paper is to identify and analyze an advanced navigation strategy for asteroid rendezvous and sample collection missions. Optimal navigation strategies for asteroid sample return missions result in low spacecraft-asteroid relative position and velocity errors.

The data used for analysis is generated through simulations of a representative design reference mission. All analysis and trade studies are based on variations of the main reference mission detailed in this section. The objective of the reference mission is to approach, rendezvous, and enter a stable orbit about the target asteroid. The analysis presented in this paper is limited to the approach and proximity operations navigation strategy. The outbound and Earth return cruise mission segments are beyond the scope of this analysis.

The reference mission target asteroid is based upon the near Earth asteroid 4660 Nereus. For this analysis, the physical properties of the asteroid were estimated using available data on Nereus and similar asteroids (Table 1). Selection of an actual asteroid as the basis of the reference target is done primarily for clarity. The outlined navigation strategy and resulting analysis, however, are not limited to this specific target asteroid and may be applicable to a diverse range of mission scenarios.

Table 1. Reference mission target asteroid physical properties

Target Asteroid Properties		
Mean Radius		0.165 km
Density		1400 kg/m^3
Mass		2.66 x 10^{10} kg
GM		1.78 x 10^{-9} km^3/s^2
Spin State	Rt. Ascension (RA)	0°
	Declination (DEC)	90°
	Spin Rate	572.19 °/d
J2 (Normalized)		0.01
C22 (Normalized)		0.001

Properties of the sample return spacecraft are presented in Table 2. The spacecraft is modeled as a spherical bus with sun-fixed solar arrays.

Table 2. Reference mission spacecraft physical properties

Spacecraft Characteristics	
Mass	1005 kg
SRP Area	13 m^2
Specular Coeff.	0.28
Diffuse Coeff.	0.06

The representative mission proximity operations navigation strategy is divided into two main segments: the asteroid approach phase and a stable orbit phase.

Asteroid Approach Phase

The Approach Phase begins after optical acquisition of the spacecraft at a distance of 2 million kilometers, approximately six weeks before closest approach. A sequence of two maneuvers, occurring four weeks after acquisition and five days before closest approach, target a distance of 10 kilometers from the asteroid on the sunward side. Each maneuver is assumed to have a 1.7% relative and 1 mm/s absolute execution error. Parameters for the Approach Phase scenario are summarized in Table 3.

Table 3. Asteroid Approach Phase scenario parameters

Asteroid Approach Phase Properties	
Scenario Start Time	09 MAR 2023 20:00:0.000
Scenario End Time	22 APR 2023 10:00:0.000
Initial Spacecraft State (Heliocentric J2000)	2.1613×10^8 km -1.6664×10^8 km -7.1068×10^7 km 8.6146 km/s 14.7709 km/s 6.8219 km/s
Initial Asteroid State (Heliocentric J2000)	2.1798×10^8 km -1.6724×10^8 km -7.1549×10^7 km 8.1026 km/s 14.9484 km/s 6.9562 km/s
Maneuver Times	06 APR 2023 20:00:0.000 17 APR 2023 10:00:0.000
Relative Execution Error	1.7%
Absolute Execution Error	1 mm/s

Ground-based measurements include DSN range and Doppler supplemented by one Delta-Differenced One Way Range (DDOR) baseline per week. DSN measurement frequency begins at four passes per week and increasing to one pass per day three weeks after asteroid acquisition. Continuous DSN measurements begin three days prior to closest approach. Additionally, spacecraft-to-asteroid range-rate and unit vector measurements are recorded every 30 minutes. Spacecraft-to-asteroid range measurements are incorporated when the spacecraft is at a relative distance

of less than 100 kilometers from the target asteroid. The tracking schedule for the Approach Phase is represented graphically in Figure 1.

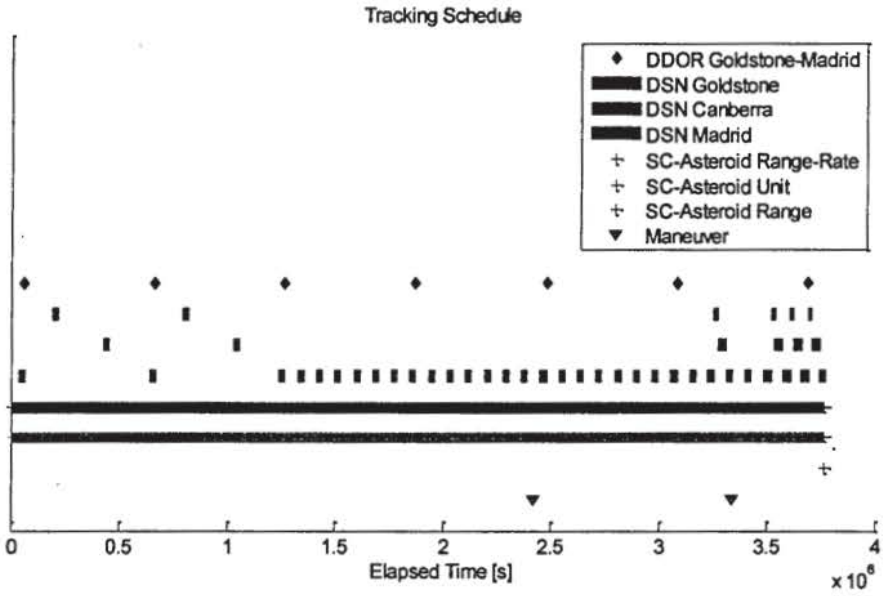

Figure 1. Reference mission graphical tracking schedule

Orbit Phase

The Approach and Orbit phases of the reference mission are analyzed separately. An Asteroid Orbit Insertion phase is assumed to occur after the asteroid approach and before the orbit phase. However, analysis of the Insertion phase is beyond the scope of this analysis.

Simulation and covariance analysis is performed for the nominal reference mission scenario. Analysis of the nominal strategy covariance and error estimates allows for navigation strategy evaluation and verification of spacecraft-asteroid relative errors. The simulation assumes the post-insertion, near-circular orbit with radius ~500 m is established by a series of small maneuvers so that the resulting orbit plane is almost in the terminator plane. For orbit stability, the motion is either retrograde or polar depending on the true orientation of the Nereus spin axis. For the asteroid property assumptions given above, the spacecraft orbit phase simulation properties are given in Table 4. The orbit scenario end time is shown for the orbit stability check, but the filter simulation will include only the first seven days after epoch.

Table 4. Spacecraft Orbit Properties about Asteroid 4660 Nereus

Orbit Phase Simulation Properties	
Scenario Start Time	23 APR 2023 12:00:0.000
Scenario End Time	23 JUL 2023 12:00:0.000
Initial Spacecraft State (Nereus centered, Nereus true equator, inertial osculating elements at start epoch)	SMA = 500 m ECC = 0.001 INC = 96.786 deg APF = 110.299 deg LAN = 60 deg TFP = 0 .0 sec Period = 12 hr

The orbit was propagated with the asteroid dynamic models for the rotating non-spherical gravity field, Solar and planetary perturbations, and solar radiation pressure (SRP) for three months to test its long-term stability. The resulting evolution of the orbit eccentricity and semi-major axis is shown in Figure 2. Note that the orbit eccentricity is fairly constant over the first 60 days of propagating indicating that the orbit is stable over the filter interval.

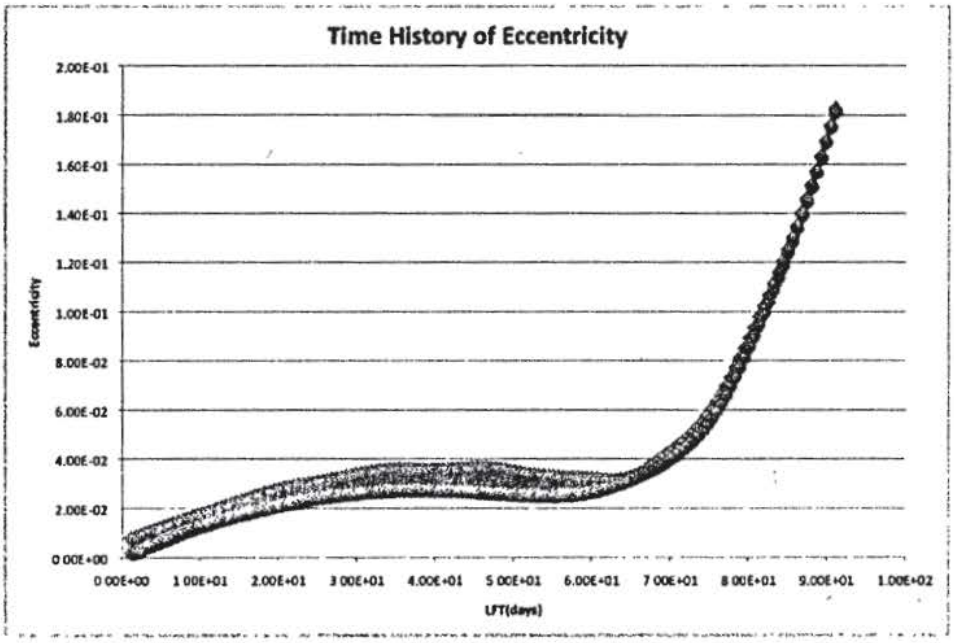

Figure 2. Evolution of spacecraft orbit eccentricity over three month propagation

The orbit geometry relative to Nereus, Earth and Sun is shown in Figure 3 for a one month propagation. The orbit displays the desired property of being near the Nereus terminator plane while maintaining a circular shape.

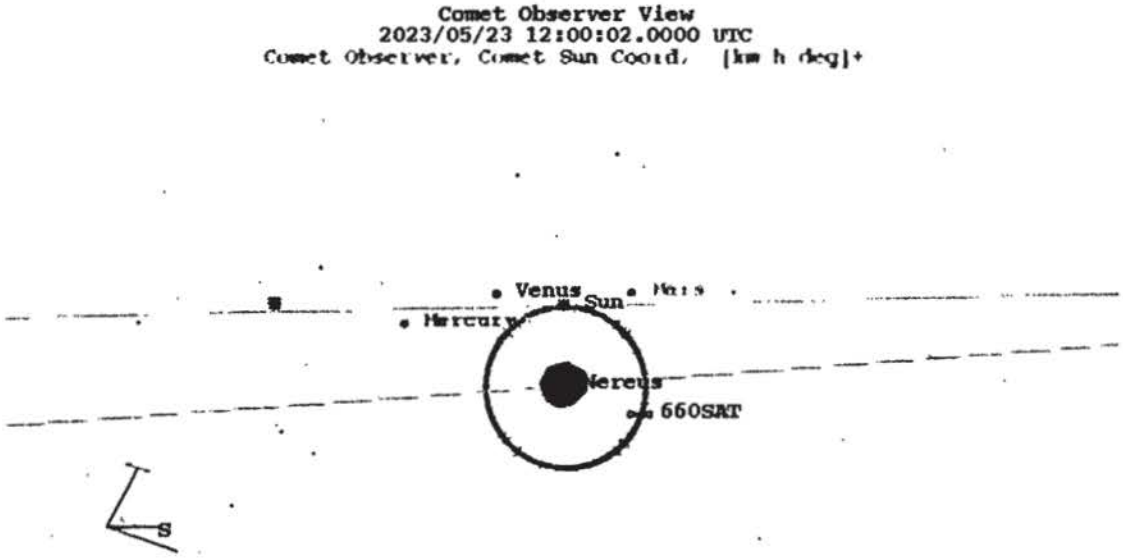

Figure 3. Simulated orbit relative to Nereus, Earth and Sun shown for one month propagation

METHODOLOGY

Asteroid Approach Phase

Covariance analysis for the Approach Phase is performed using data provided by simulations using the Orbit Determination Toolbox (ODTBX) Matlab toolbox. ODTBX was developed by the Navigation & Mission Design branch at NASA Goddard Space Flight Center for use in mission design and analysis. Data simulation and analysis utilized the sequential estimator function provided in ODTBX.

The filter states were selected to analyze the relative covariance and estimation error associated with the relative position and velocity of the spacecraft with respect to the target asteroid. The first six states represent the relative position and velocity of the true asteroid with respect to the reference trajectory provided by a SPICE file, accessed through the Jet Propulsion Laboratory (JPL) Horizons interface. States seven through twelve are defined as the relative position and velocity of the spacecraft with respect to the true asteroid state.

The thirteenth and fourteenth are modeled as consider states with a Gaussian random walk. The thirteenth state represents the target asteroid gravitational parameter (GM). The fourteenth state, known as the SRP scale factor, represents the difference in mass, area, and coefficient of reflectivity between the spacecraft and asteroid, and is used in calculating relative SRP forces. The estimated states are listed in Table 5.

Table 5. Description of estimated states

Estimated State	Description
Solve-For States	
Target Asteroid Relative State (6)	Relative position and velocity (J2000) of the true target asteroid relative to the reference state provided by a JPL SPICE file
Spacecraft-Asteroid Relative State (6)	Relative position and velocity (J2000) of the spacecraft with respect to the true asteroid state
Consider States	
Asteroid GM	Gravitational Parameter of the target asteroid
Solar Radiation Pressure (SRP) Scale Factor	Scale factor representing the difference in SRP forces acting on the target asteroid and spacecraft

Measurement Model

For simplicity, the scope of analysis of this paper is limited to six measurement types: Deep Space Network range and Doppler, Delta-Differenced One Way Range, radiometric range-rate, optical, and laser ranging. Table 6 outlines each of the actual measurement types and the associated simulated measurements used for analysis.

Table 6. Actual and simulated measurement descriptions

Actual Measurement Type	Simulated Measurement
Ground-Based	
DSN Range	DSN Ground Station to spacecraft range
DSN Doppler	DSN Ground Station to spacecraft range-rate
Delta-Differenced One Way Range (DDOR)	DSN Ground Station (2) to spacecraft DDOR
Spacecraft-Based	
Radiometric	Spacecraft to asteroid range-rate
Optical	Spacecraft to asteroid line-of-sight angles
Laser Range	Spacecraft to asteroid range (maximum range of 100 km)

Estimator

The ODTBX sequential estimator function is based on the sequential estimator design presented by Markley[1, 2] and Carpenter[3]. The ODTBX version of the estimator utilizes a dynamics and measurement model function to return the estimated state and covariance over a specified time interval.

The resulting state and covariance estimates for the representative mission are used for spacecraft-asteroid relative error and covariance analysis.

Orbit Phase

The orbit phase covariance analysis used the MIRAGE software set developed by JPL. The filter assumptions for estimated and considered parameters are shown in Table 7. The filter parameters were chosen based on NASA's NEAR mission experience[4]. The simulated tracking data schedule for one week in the orbit phase is shown in Figure 4.

Table 7. Orbit phase covariance analysis assumptions

Baseline Covariance Analysis Assumptions	
Estimated Parameters	**A-priori Uncertainty**
Spacecraft State	50 km, 30 m/s
Solar pressure	Effective cross section 5 m^2, 1σ Momentum transfer coefficient 1.5 (±10%)
Stochastic acceleration	1.0×10^{-12} km/s constant bias, 1σ 7.5×10^{-11} km/s variable, 1σ 10 day time constant, 2 day batch size
Maneuver Execution Errors	2% (magnitude and pointing) + 1 mm/s (magnitude), all 3σ
Planetary and Asteroid Ephemerides	DE418 with correlated covariances and Nereus diagonal sigmas provided by JPL's Solar System Dynamics group

Consider Parameters	
Station locations	Correlated covariance determined from VLBI processing
UT1 and polar motion	.34 msec, 15 nrad.
Troposphere (wet and dry)	4 cm, 1 cm
Ionosphere	.5 x 10^{17} elec/m^2

Data Type	Data Weight
2-Way Doppler	0.1 mm/s
2-Way Range	50 m
Delta-DOR	0.6 ns (20 cm on each baseline)
OpNav	1 pixel (25 μrad)

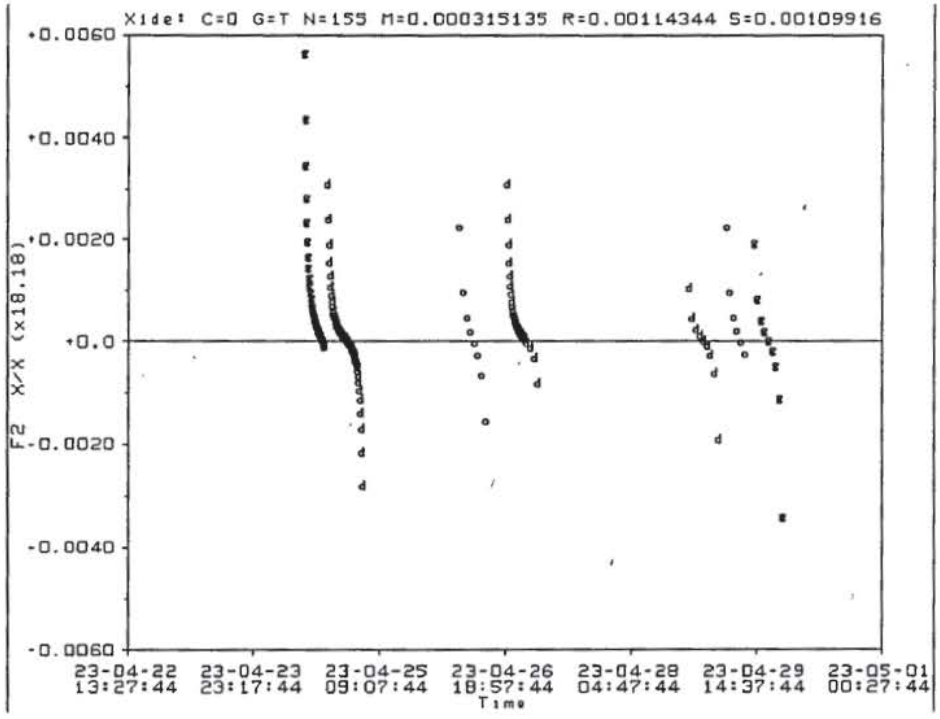

Figure 4. Simulated tracking for orbit phase

RESULTS

Approach Phase

Figure 5 represents the asteroid relative position errors associated with the true and formal states. During the intermittent DSN tracking phase, asteroid position errors and covariance remains relatively large. Decreases in the covariance can be observed after DDOR measurements and are consistent with an increase in plane-of-sky asteroid position accuracy[5].

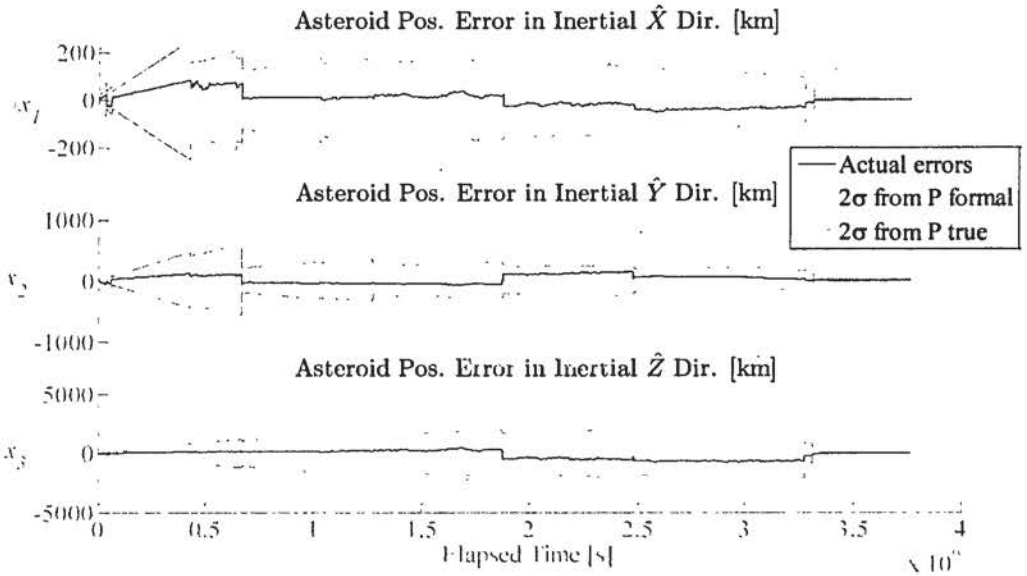

Figure 5. Asteroid relative position errors and associated true and formal covariance

Contributions of the a-priori, measurement, process, and maneuver execution noise to the asteroid relative X direction inertial position covariance is shown in Figure 6. The presence of large a-priori contributions to the covariance during the intermittent DSN phase implies that the asteroid state is not fully observable. Covariance analysis of the Y and Z components of the asteroid relative position yielded similar results.

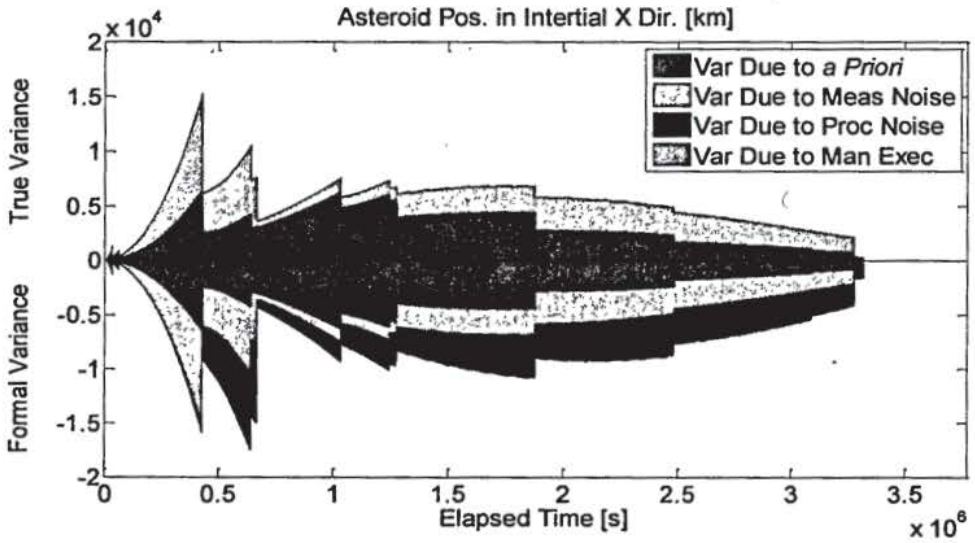

Figure 6. Asteroid position in the inertial X direction variance sandpile plot

The asteroid relative position error and covariance decrease dramatically following the first continuous DSN tracking segment, as seen in both Figure 5 and Figure 6.

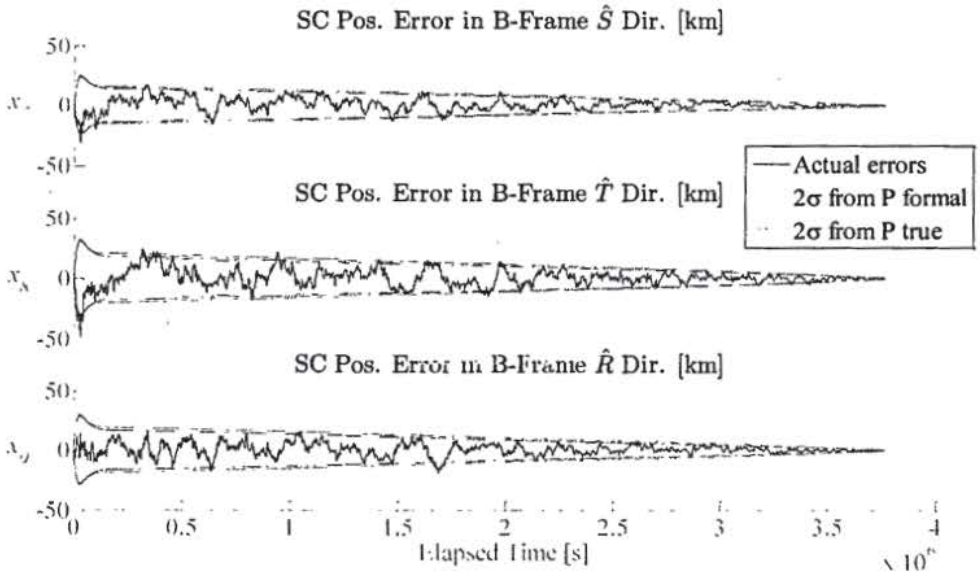

Figure 7. Spacecraft relative position errors and associated true and formal covariance

Results from the spacecraft relative position error analysis are presented in Figure 7. Spacecraft relative position error and covariance steadily converge for the duration of the simulation. Optical and range-rate measurements of the asteroid from the spacecraft allow a reduced DSN tracking schedule while maintaining spacecraft relative state full observability and accuracy.

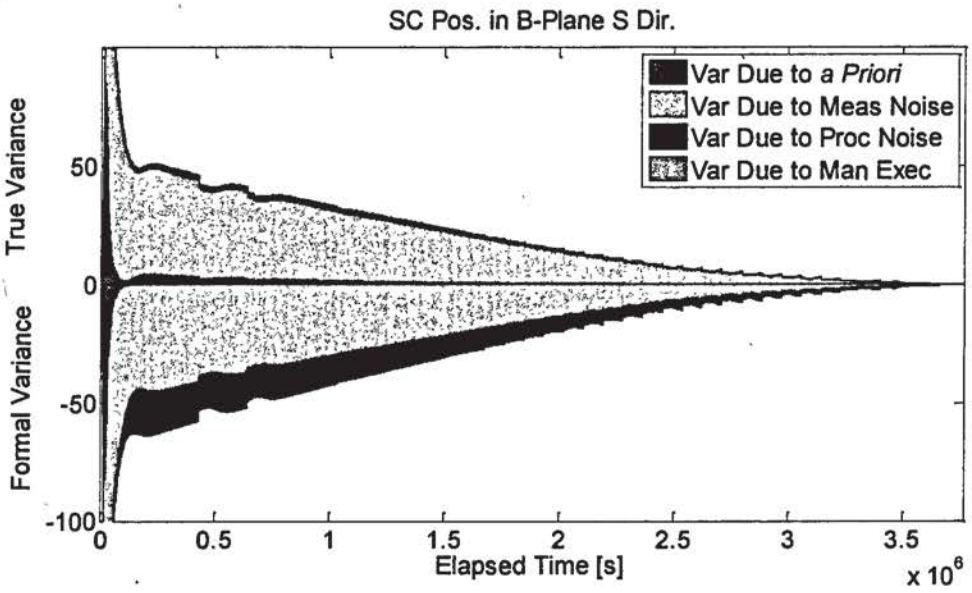

Figure 8. Spacecraft position in the B-Plane S direction variance sandpile plot

Examination of the spacecraft B-Plane S position covariance contributions (Figure 8) reveals a slightly larger contribution of a-priori noise in the truth compared to the formal covariance. This is evidence of the sensitivity of the spacecraft position to the consider parameters, which are not incorporated in the formal analysis. The maneuver execution error covariance partition is not apparent in Figure 8 and appears to be insignificant compared to the other partitions. Similar results were observed in the spacecraft relative position in the B-Plane T and R directions.

Further investigation into the sensitivity of the consider parameters is performed by analyzing the sensitivity matrix using a sensitivity mosaic. The section of the sensitivity mosaic corresponding to the spacecraft relative state is presented in Figure 9. A slight sensitivity to the asteroid GM and the SRP scale factor is seen in the spacecraft relative position. The spacecraft position in the B-Frame R direction has a slightly negative sensitivity to both consider parameters. The spacecraft position in the B-Frame S and T direction had a slightly positive sensitivity to SRP only.

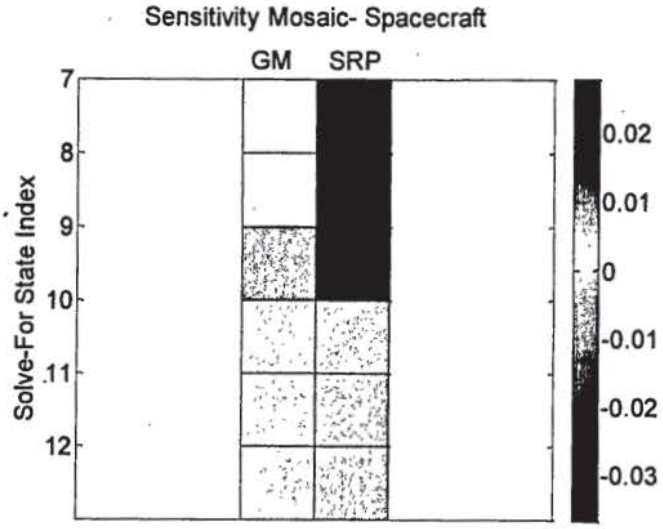

Figure 9. Sensitivity of the spacecraft relative state to GM and SRP Scale Factor consider parameters

A plot of the spacecraft relative position error ellipse projected in the asteroid B-Frame at the time of closest approach is presented in Figure 10. Analysis of Figure 10 suggests the navigation strategy is capable of estimating the spacecraft relative state to meter-level accuracy.

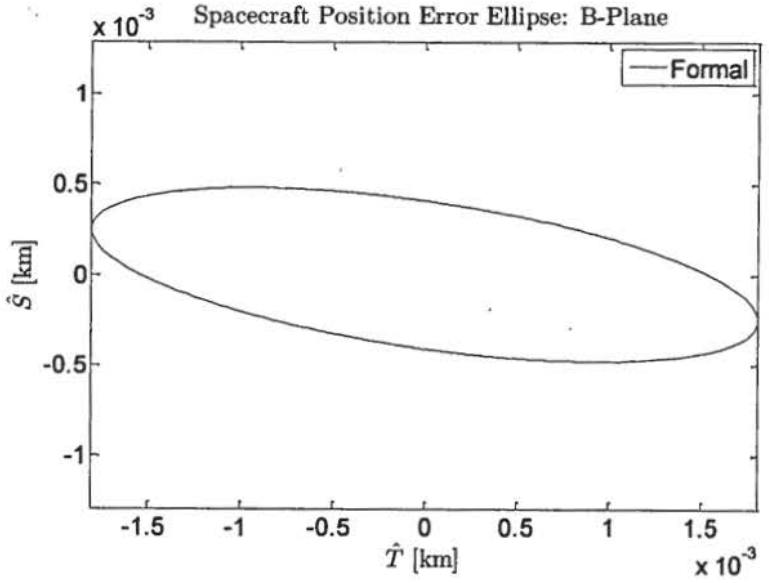

Figure 10. Spacecraft relative position error ellipse projected in the B-Frame

Although spacecraft relative position truth-estimate difference errors remained relatively low during the continuous DSN tracking segment and at the time of closest approach, the difference between the true and desired trajectories were unacceptably large. In initial simulations, the DSN tracking frequency did not increase until after the second and final maneuver. Subsequently, because the targeting maneuvers are based on the estimated position, large errors were introduced to the true state causing the spacecraft to be hundreds of kilometers from the desired point of closest approach. Simulations used to generate results for this analysis were corrected with a modified tracking schedule that increase DSN tracking before the final maneuver to reduce asteroid and spacecraft relative position and velocity errors.

Another consideration for the difference in the true and desired trajectory is the uncertainty of the consider parameters. Table 8 presents the spacecraft relative position with respect to the asteroid at the time of closest approach for the desired, true, and modified true trajectory. The modified true trajectory is generated without the GM and SRP scale factor consider parameters.

Table 8. Asteroid-centered J2000 Cartesian position of the spacecraft at the point of closest approach for the desired, true, and modified true trajectory

	Desired	True	Modified True
X	-9.0412 km	-5.3719 km	-7.5308 km
Y	3.9642 km	61.2767 km	8.2858 km
Z	1.6188 km	-47.3985 km	-9.6355 km

The modified true trajectory without consider parameters comes significantly closer to the desired point of closest approach compared to the true trajectory. This demonstrates the dependence between the desired-true trajectory difference and the knowledge of the consider parameters.

Orbit Phase

The orbit phase position and velocity uncertainties are shown in Figure 11 and Figure 12 for the seven day filter arc. The position and velocity components of uncertainty are shown in a Cartesian frame with one component (c_sig_**V**) oriented along the instantaneous velocity vector, another component (c_sig_**H**) oriented parallel to the orbit angular momentum vector, and the third component (c_sig_**V**x**H**) oriented parallel to the cross product of velocity and angular momentum vectors. For the near-circular obit considered over the filter interval, the **V**x**H** component is almost in the radial direction from the center of mass of Nereus to the spacecraft. Similarly, the **V** component is in the down track direction and the **H** component is out-of-plane or cross track. Note that the uncertainty in the velocity direction (down track) is the largest and the cross track uncertainty is the smallest, which is typical when the orbit plane is oriented more face-on to the line-of-sight from Earth as it is here (see Figure 3).

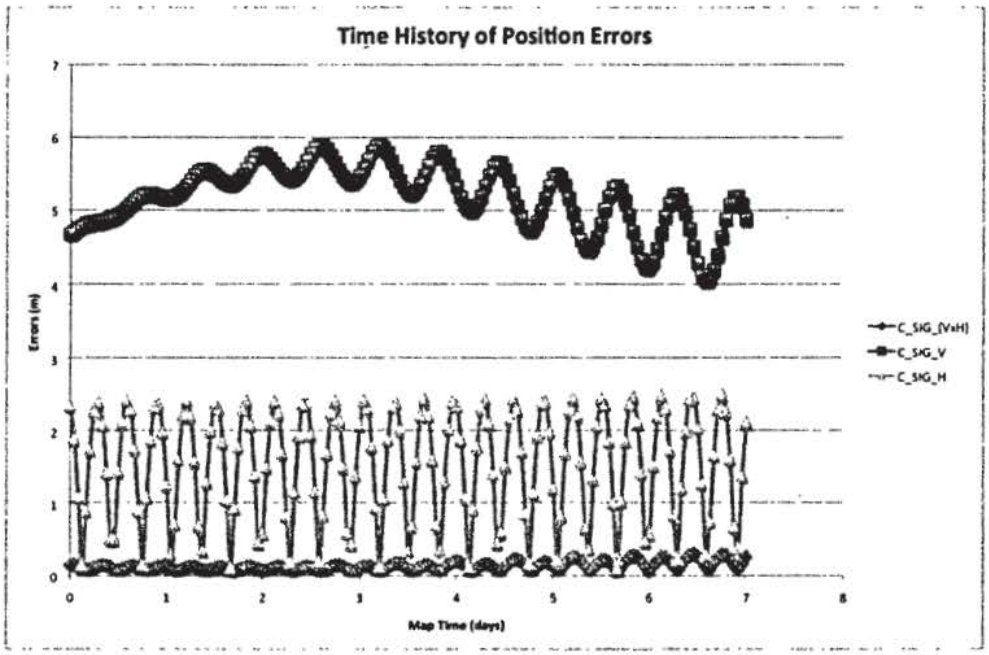

Figure 11. Orbit phase position uncertainty

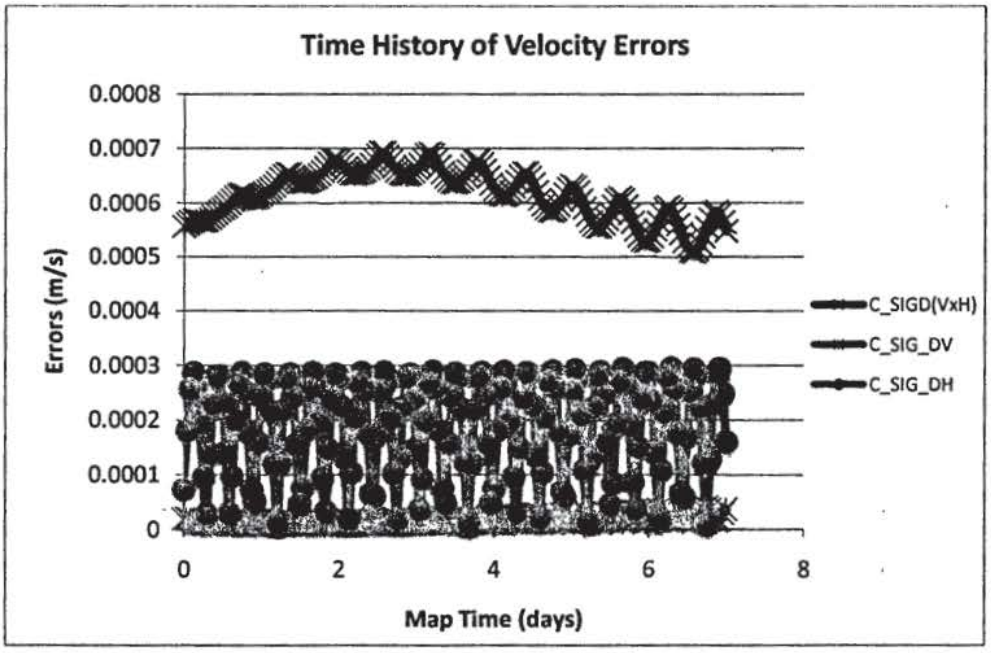

Figure 12. Orbit phase velocity uncertainty

The corresponding uncertainty in the osculating orbit eccentricity is shown in Figure 13.

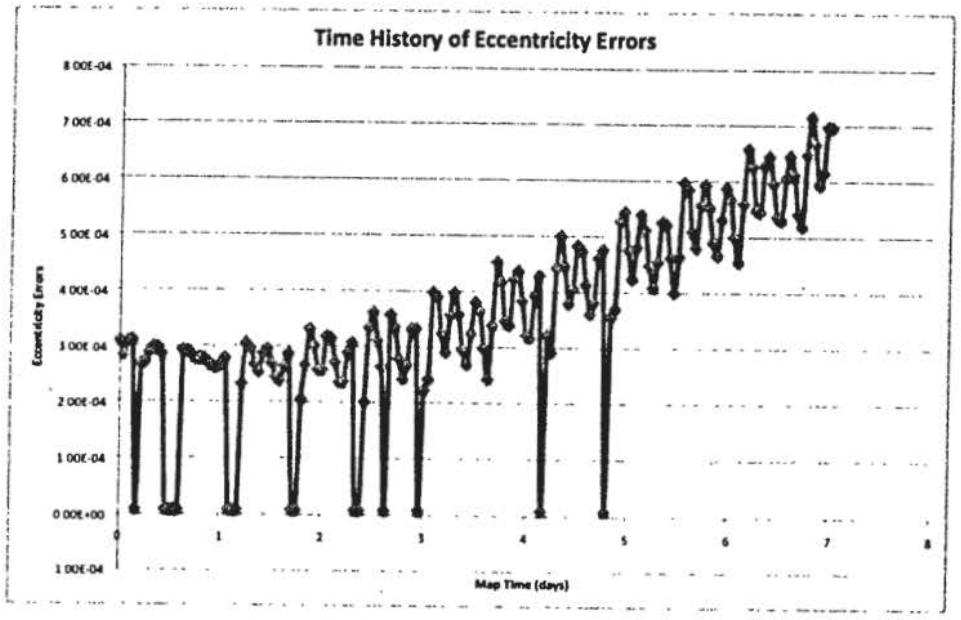

Figure 13. Uncertainty in orbit eccentricity

The corresponding errors along the semi-major axis are shown in Figure 14.

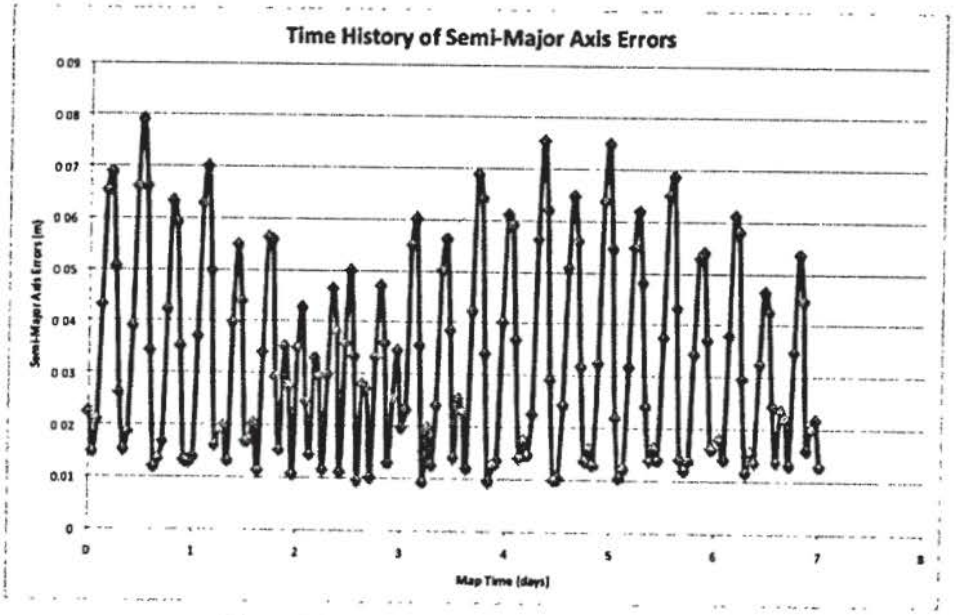

Figure 14. Uncertainty along semi-major axis

CONCLUSION

Results of current error and covariance analysis confirm the effectiveness of the reference mission scenario to reduce spacecraft-asteroid relative errors at the time of closest approach to meter-level accuracy. Autonomous spacecraft-based optical and range-rate measurements allowed for a reduced DSN tracking schedule during the intermittent phase while maintaining relatively low spacecraft state error and covariance. However, large errors between the desired and true trajectories suggest sensitivity to the GM and SRP consider states. Large asteroid and spacecraft relative errors at maneuver times also contribute to the desired-true trajectory difference and can be propagated into the trajectory if present at the time of the targeting maneuver calculation. In this study, increasing the DSN tracking frequency before the target maneuver Δv calculation resolved this issue.

The orbit phase analysis shows that the assumed spacecraft, orbit and filter characteristics will also result in meter-level accuracies relative to the asteroid. This level of accuracy is sufficient to perform proximity operations about an asteroid like 4660 Nereus.

FUTURE WORK

Future analysis will focus on improving the fidelity of the dynamics and measurement models. Assumptions made for measurement models, such as unit vector measurements to simulate optical and landmark tracking, will be improved and eventually replaced with more accurate representations. Incorporating different states, including additional consider and bias parameters, could provide additional insight to the sensitivity of the navigation solution. Approach phase Monte Carlo runs are required to improve the accuracy of the simulation. Adding asteroid fly-by and reconnaissance segments to the navigation mission timeline could improve asteroid gravity, shape, and spin models and reduce the uncertainty in GM and SRP scale factor.

Variations of the nominal reference mission and trade studies could provide further navigation strategy optimization and identify ways of reducing the reliance on tracking schedule resources while maintaining required levels of accuracy. Specifically, including tracking such as optical images of landmarks or altimetry with an on board orbit determination capability could greatly reduce the ground-based tracking required. Such a capability could be gradually enabled once the fundamental physical characteristics of the asteroid and the spacecraft orbit precision were established by using more conventional ground-based techniques.

REFERENCES

[1] MARKLEY, F. L., SEIDEWITZ, E., and NICHOLSON, M., "A General Model for Attitude Determination Error Analysis", NASA Conference Publication 3011: Flight Mechanics/Estimation Theory Symposium, May 1988, (pp.3–25).

[2] MARKLEY, F. L., SEIDEWITZ, E., and DEUTSCHMANN, J., "Attitude Determination Error Analysis: General Model and Specific Application", Proceedings of the CNES Space Dynamics Conference, Toulouse, France, November 1989, (pp. 251–266).

[3] CARPENTER, J. R. and MARKLEY, F. L., "Generalized Linear Covariance Analysis," Proceedings of the F. Landis Markley Astronautics Symposium, edited by J. L. Crassidis et al., Vol. 132 (CD–ROM Supplement) of Advances in the Astronautical Sciences, American Astronautical Society, Univelt, 2008.

[4] WILLIAMS, B. G., et al, "Navigation for NEAR Shoemaker: the First Spacecraft to Orbit an Asteroid," AAS/AIAA Astrodynamics Specialist Conference, Quebec City, Quebec, Canada, July 30-August 2, 2001, Paper AAS 01-371.

[5] MARTIN-MUR, T., et al., "Use of Very Long Baseline Array Interferometric Data for Spacecraft Navigation", Proceedings of International Symposium on Space Technology and Science, 2006-d-50, 2006.